

## Hydrogen Photoevolution from Water-Methanol on Ru/TiO<sub>2</sub>

Andrzej Sobczynski\*, Teresa Jakubowska, and Stanislaw Zielinski

Department of Chemistry, Adam Mickiewicz University, PL-60-780 Poznan, Poland

**Summary.** *"In situ"* ruthenium photodeposition on anatase TiO<sub>2</sub> was found to be an efficient method of obtaining Ru/TiO<sub>2</sub> powders highly active in hydrogen photoevolution from water-methanol. The efficiency of the catalyst was higher when the TiO<sub>2</sub> powder was subjected to a cation exchange prior to illumination in water-methanol. Reaction conditions were optimized; it was found that the most active sample was TiO<sub>2</sub> covered with 0.75 wt% Ru. Anatase TiO<sub>2</sub> itself was found to be porous with an average cylindrical pore radius of 37 Å. SEM and electron microprobe analysis showed that the photodeposition of ruthenium on the porous substrate resulted in a nonhomogeneous distribution on the TiO<sub>2</sub> surface. The size of ruthenium islets seems to influence the stability of Ru/TiO<sub>2</sub> catalysts in hydrogen photoevolution from water-methanol.

**Keywords.** Photocatalysis; Ruthenium; Titania.

### Photoevolution von Wasserstoff aus Wasser-Methanol auf Ru/TiO<sub>2</sub>

**Zusammenfassung.** Es wurde festgestellt, daß die „*in situ*“ Photodepositierung von Ruthenium auf Anatas-TiO<sub>2</sub> eine effiziente Methode darstellt, um Ru/TiO<sub>2</sub>-Pulver herzustellen, das eine hohe Aktivität bei der Photoevolution von Wasserstoff aus Wasser-Methanol besitzt. Die Effizienz des Katalysators war höher, wenn das TiO<sub>2</sub>-Pulver vor der Bestrahlung einem Kationenaustausch unterworfen wurde. Die Reaktionsbedingungen wurden optimiert; TiO<sub>2</sub>, bedeckt mit 0.76 Gew% Ru, zeigte sich als aktivster Katalysator. Anatas-TiO<sub>2</sub> selbst erwies sich als porös mit einem mittleren zylindrischen Porenradius von 37 Å. Mittels SEM und Mikrosondenanalyse wurde festgestellt, daß die Photodepositierung von Ruthenium auf dem porösen Substrat eine nichthomogene Verteilung auf der TiO<sub>2</sub>-Oberfläche ergibt. Das Ausmaß und die Größe der Ruthenium-Anhäufungen scheinen die Stabilität von Ru/TiO<sub>2</sub>-Katalysatoren bei der Photoevolution von Wasserstoff aus Wasser-Methanol zu beeinflussen.

### Introduction

Noble metals are of great interest because of their high activity in the mediation of hydrogen evolution on irradiated semiconductors. Different preparation methods of metal-covered titania have been described [1–18] and comparisons between them have been done [19, 20]. The most widely used was wet impregnation followed by reduction at elevated temperatures [1]. Some modifications of this method have been also employed [2]. The ease of reducibility of noble metal ions allowed to apply a photodeposition method [3–11]. The formation of metal deposits was

efficient when organic compounds such as acetate [4, 5], alcohols [6, 8–11] and others [7] were added to water prior to irradiation. The photodeposition of noble metals on semiconductors found an application as an efficient method of recovery of precious metals from diluted solutions [12, 13]. Ultrafine deposits of platinum and other precious metals on  $\text{TiO}_2$  have been obtained by mixing the substrate with a separately prepared sol of an appropriate metal [7, 14–16]. The thermal decomposition of noble metal cluster compounds like  $\text{Rh}_6(\text{CO})_{16}$  or  $\text{Ru}_3(\text{CO})_{12}$  also provides another method of preparing and controlling metal deposits on  $\text{TiO}_2$  [17, 18].

It was reported previously [10, 11] that “*in situ*” photodeposition of platinum on  $\text{TiO}_2$  resulted in highly efficient hydrogen photoproduction from water in the presence of methanol as a sacrificial electron donor. The photodeposition reaction was optimized and the influence of some factors like *pH*, concentration of different electrolytes, and platinum preadsorption from a solution of hexachloroplatinic acid [a cation exchange between the Pt(IV) species and surface OH groups of anatase] was described.

In the present paper, an “*in situ*” photodeposition of ruthenium on titania from a ruthenium(III) chloride solution was studied along with the textural properties of  $\text{TiO}_2$  as well as the ruthenium distribution on the substrate. It was found that the optimum ruthenium coverage on  $\text{TiO}_2$  was 0.76 wt% and that the preadsorption of  $\text{Ru}^{3+}$  ions on the  $\text{TiO}_2$  surface resulted in a greater efficiency of hydrogen production from water-methanol. SEM and electron microprobe analysis showed that although the entire surface of the  $\text{TiO}_2$  particle was covered with ruthenium, the metal distribution was not homogeneous: separate metal islands could be seen in both analyses.

## Experimental

Titanium dioxide was prepared in the manner described previously [10] by the hydrolysis of titanium tetrachloride (Fluka) in water. The product, after calcination for 4 h at 637 K had a BET specific surface area of  $122 \text{ m}^2 \text{ g}^{-1}$  and was pure anatase by XRD.

Pore size distribution was studied using a method described by Cranston and Inkley [21] with a computer analysis of a nitrogen adsorption isotherm (77 K). The measurements were performed on a Gravimat-Sartorius Model 4133 vacuum microbalance. Prior to measurements, the sample (100 mg) was outgassed at  $10^{-6}$  Torr at 570 K until a constant weight was achieved.

Hydrogen evolution experiments were performed in a bulb-shape Pyrex reaction cell with a volume of about 120 ml under flowing argon ( $500 \text{ ml h}^{-1}$ ). The cell was placed in a Pyrex water bath which was maintained at  $298 \pm 1 \text{ K}$ . Irradiation was carried out through the side wall of the cell with a 180 W medium pressure Hg lamp. Evolving hydrogen was analysed by GC [10].

Ruthenium photodeposition was carried out “*in situ*” in a reaction cell using a  $\text{RuCl}_3$  solution. About 20 h prior to irradiation 0.1 g  $\text{TiO}_2$  was mixed with an appropriate amount of ruthenium trichloride solution (and sonicated for 30 minutes) in order to achieve, at least in part, a cation exchange between the OH surface groups of  $\text{TiO}_2$  and  $\text{Ru}^{3+}$  ions. The catalyst slurry was transferred to the reaction cell, where 10 ml of methanol was added. The cell was then filled with water up to 100 ml so that the volume ratio of water to methanol was 10 : 1. After the reaction mixture had been deaerated in flowing argon (usually 2 h) illumination was started. The catalyst was sustained in a slurry using a Pyrex covered magnetic stirrer bar. Evolving hydrogen was removed from the reaction cell in a stream of argon ( $500 \text{ ml h}^{-1}$ ) and analysed by GC at 30 minute intervals.

The incident light flux was  $12.9 \cdot 10^{-2} \mu\text{mol quanta s}^{-1}$ , as measured by an uranyl-oxalate actinometer [10].

SEM analysis was performed using a JEOL Model JSM-50 apparatus. The ruthenium distribution on the surface of TiO<sub>2</sub> was analysed by an electron microprobe analysis using a microsound JXA-50A coupled with the JEOL JSM-50A scanning electron microscope.

## Results and Discussion

The titanium dioxide used in this study was taken from the same bath as described previously [10]. XRD analysis showed that it was pure anatase. The specific surface area was 122 m<sup>2</sup> g<sup>-1</sup>. The sample was found to be porous with an average pore radius of 37 Å and a total pore volume of 0.24 cm<sup>3</sup> g<sup>-1</sup>. The slope of nitrogen adsorption-desorption isotherm (77 K) indicated that the pores were cylindrical. A detailed description of the surface structure of different TiO<sub>2</sub> samples will be given elsewhere [22].

In the “*in situ*” method of ruthenium photodeposition the titanium dioxide first was subjected to a cation exchange with a solution of ruthenium(III) chloride. The adsorption of Ru<sup>3+</sup> ions could be observed visually; after several hours, the white TiO<sub>2</sub> particles turned brown-gray and the solution above the catalyst became colorless. After about 20 h, the slurry of TiO<sub>2</sub> in the RuCl<sub>3</sub> solution was mixed with methanol-water, deaerated in a stream of argon and illuminated with light from a 180 W medium pressure Hg lamp.

Illumination of anatase with a light of energy equal to or higher than the band gap energy (3.2 eV) results in electrons being excited to the conduction band (CB), leaving holes in the valence band (VB). The excited electrons have sufficient energy to reduce both Ru(III) to a metal and H<sup>+</sup> ions from water to gaseous hydrogen. The holes in the VB are capable to oxidize methanol to HCHO, CO or CO<sub>2</sub> [11, 23–27].

Thus, at the beginning of illumination, two competitive reduction processes occur on the surface of illuminated titania: deposition (reduction) of ruthenium and hydrogen production. Only hydrogen evolution should occur after all of the Ru<sup>3+</sup> has been reduced.

**Table 1.** Ru coverages on titania, rates and quantum yields of hydrogen evolution from a water-methanol

Amount of Ru		H <sub>2</sub> rate <sup>a</sup> μmole h <sup>-1</sup>	Quantum yield <sup>b</sup> %
wt%	atoms m <sup>-2</sup> · 10 <sup>17</sup>		
0.08	0.37	16.9	7.2
0.15	0.74	19.1	8.2
0.23	1.11	23.8	10.2
0.31	1.47	26.3	11.3
0.38	1.84	28.4	12.2
0.53	2.58	33.5	14.4
0.76	3.69	37.4	16.1
1.14	5.53	18.7	8.1
1.52	7.37	18.4	7.9

<sup>a</sup> The average hydrogen rate after 3 h.

<sup>b</sup> [(μmole H<sub>2</sub> s<sup>-1</sup>) · 2/μmol quanta s<sup>-1</sup>] · 100%.

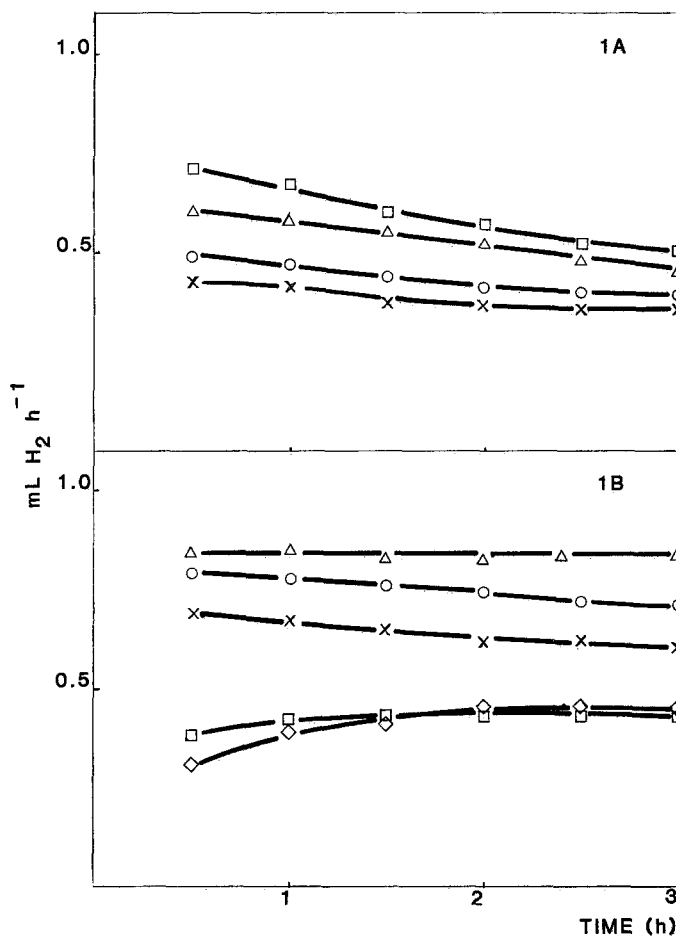


**Fig. 1.** Hydrogen evolution rates vs. time for different Ru coverages. **A:**  $\times$  0.08 wt%;  $\circ$  0.15 wt%;  $\triangle$  0.23 wt%;  $\square$  0.31 wt%. **B:**  $\times$  0.38 wt%;  $\circ$  0.53 wt%;  $\triangle$  0.76 wt%;  $\square$  1.14 wt%;  $\diamond$  1.52 wt%

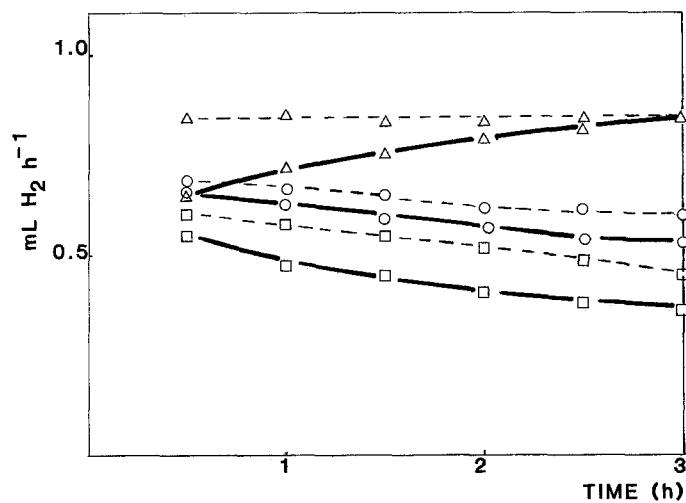


**Fig. 2.** Hydrogen evolution rates vs. time for different Ru coverages. Solid lines:  $\text{Ru}^{3+}$  was not preliminary adsorbed; dashed lines:  $\text{Ru}^{3+}$  adsorption preceded the hydrogen evolution experiments.  $\triangle$  0.76 wt% Ru;  $\circ$  0.38 wt% Ru;  $\square$  0.23 wt% Ru

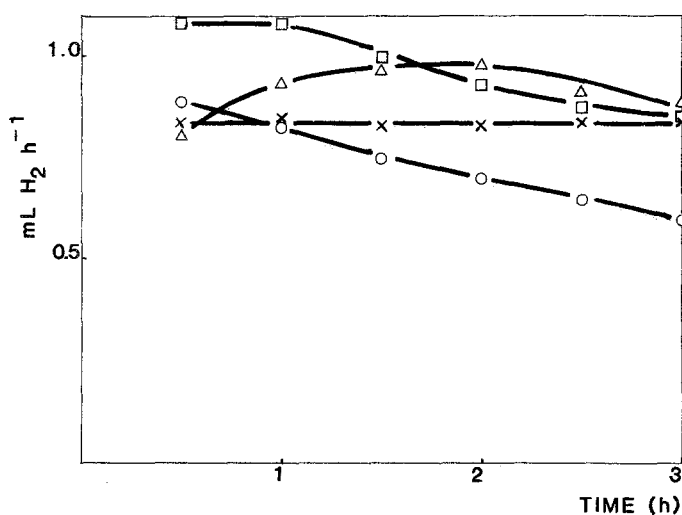


**Fig. 3.** Hydrogen evolution rates vs. time for different *pH* of a water-methanol solution. Ru coverage 0.76 wt%: × *pH* 3.9; ○ *pH* 7.5; □ *pH* 11.3; Δ *pH* 14.0

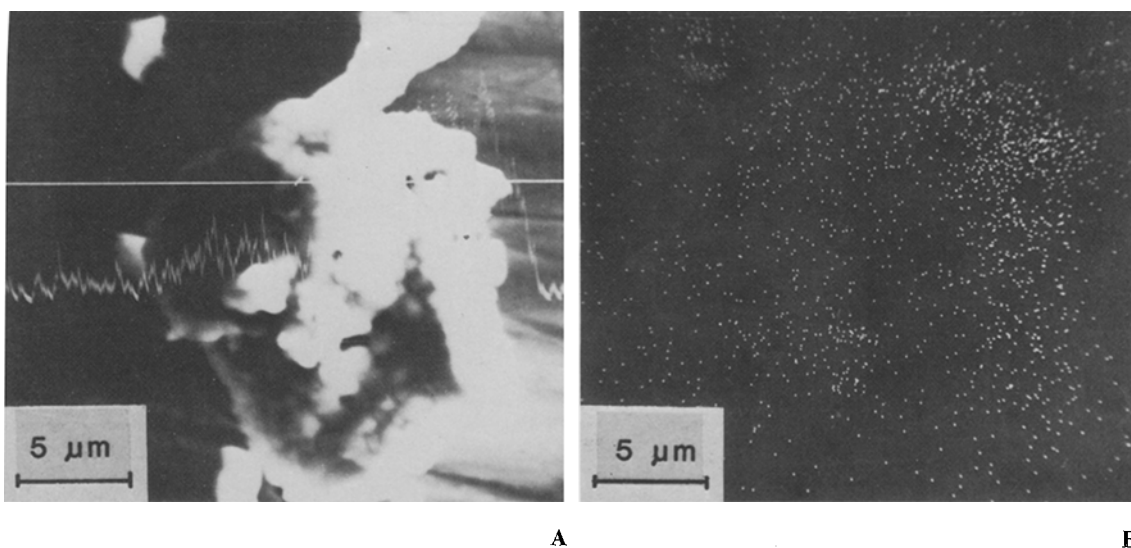


**Fig. 4.** SEM and electron microprobe analysis of 0.76 wt% Ru/TiO<sub>2</sub>. Magnification 4000 ×; **A**: secondary electron image and electron microprobe analysis along the depicted axis; **B**: line-by-line electron microprobe analysis

In Table 1 the average reaction rates (after 3 h of illumination) and the quantum yields of hydrogen production for various ruthenium coverages are listed. Time dependences of the reaction rates are shown in Figs. 1 A and 1 B.

The following conclusions can be drawn from the results shown in Table 1 and Fig. 1:

1. TiO<sub>2</sub> with 0.76 wt% of deposited ruthenium shows both the highest activity and best stability for hydrogen photoevolution from water-methanol. The quantum yield of the process (the ratio of the amount of hydrogen atoms produced to

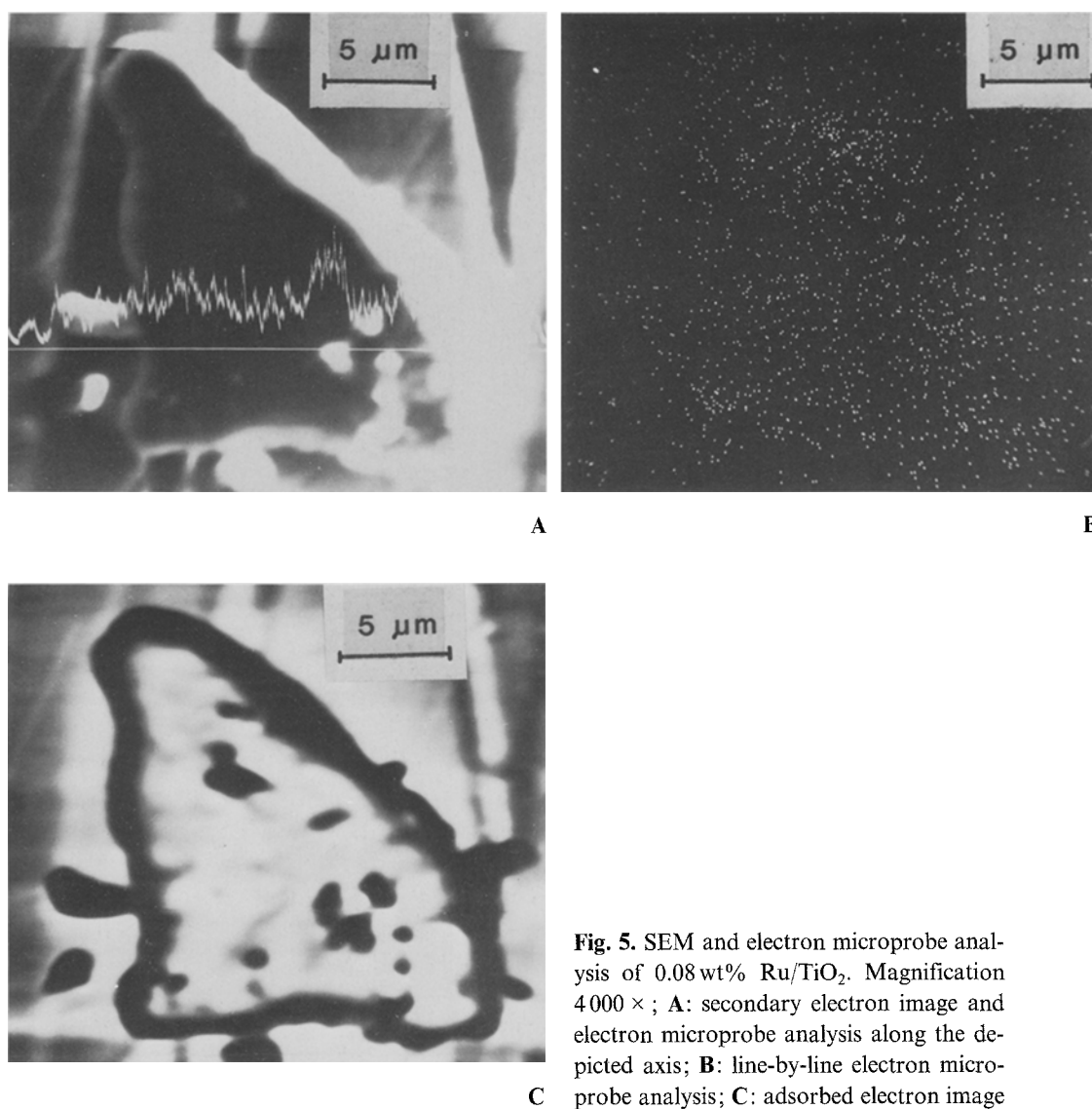


**Fig. 5.** SEM and electron microprobe analysis of 0.08 wt% Ru/TiO<sub>2</sub>. Magnification 4000 × ; **A:** secondary electron image and electron microprobe analysis along the depicted axis; **B:** line-by-line electron microprobe analysis; **C:** adsorbed electron image

the amount of quanta of incident light × 100%) was found to be 16.1% (see Table 1). The coverage of the surface by ruthenium is about ten times less than the expected monolayer coverage [28].

2. For Ru coverages smaller than 0.76 wt% the hydrogen production activity is not stable over time. Although it is rather high at the beginning of illumination and with the value near that of 0.76 wt% Ru/TiO<sub>2</sub>, it decreases drastically with time.

3. For Ru coverages higher than 0.76 wt% the activity increases with time and attains a steady state value after about 1.5 h of illumination. However, hydrogen production rates are about two times lower than that of 0.76 wt% Ru/TiO<sub>2</sub>.

For Ru contents less than 0.76 wt% the relatively high ratios of hydrogen photoproduction at the beginning of illumination (the absence of an increasing

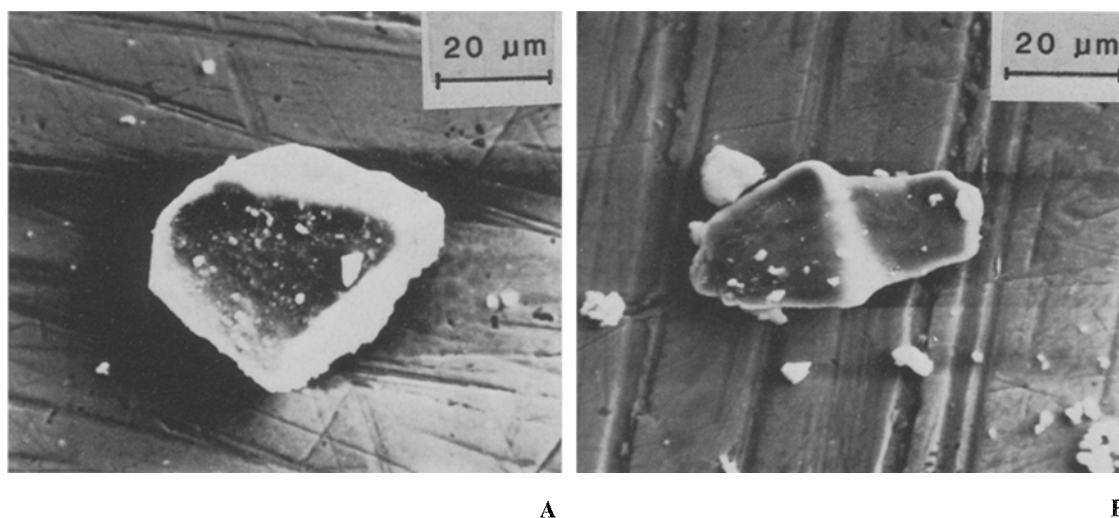


**Fig. 6.** Secondary electron image (magnification 1000 ×); **A:** 0.76 wt% Ru/TiO<sub>2</sub>; **B:** 0.08 wt% Ru/TiO<sub>2</sub>

curve) shows that all of the Ru<sup>3+</sup> ions are reduced within 0.5 h. The very fast Ru<sup>3+</sup> reduction is a result of the complete adsorption of ruthenium(III) on the TiO<sub>2</sub> surface. For Ru contents greater than 0.76 wt%, the lower hydrogen production at the early stage of illumination is indicative for its competition with Ru<sup>3+</sup> reduction. Here Ru<sup>3+</sup> ions are not totally adsorbed by TiO<sub>2</sub> and they are not reduced until they reach the surface of titania. The rather low yield of hydrogen on these samples can be caused by a “screening effect” of the TiO<sub>2</sub> surface by the high amount of metal deposition which lowers the intensity of the light beam reaching the surface or it can result from the negative effect of the metal on the separation of charges as it was predicted by Pichat [26].

To support our hypothesis concerning the influence of ruthenium(III) adsorption, hydrogen photoevolution was studied from Ru<sup>3+</sup>-TiO<sub>2</sub> slurry in water-methanol without preliminary ruthenium adsorption on titania. However, it was expected that some of the Ru<sup>3+</sup> ions would adsorb on TiO<sub>2</sub> while the solution was deaerated for two hours. The rate of hydrogen photoevolution vs. time is shown in Fig. 2. We found that the shape of the curve for 0.76 wt% ruthenium loading depends on the Ru<sup>3+</sup> adsorption preceding illumination of the slurry. For the sample not subjected to a cation exchange, the increasing curve indicates the competition between ruthenium(III) reduction and hydrogen photoproduction. For lower Ru coverages (0.22 and 0.37 wt%) all of the Ru<sup>3+</sup> ions were probably adsorbed on TiO<sub>2</sub> during the 2 h of preliminary deaeration.

The decrease of hydrogen production ratios with time for a Ru coverage lower than 0.76 wt% (see Fig. 1 A) and the stability for higher ruthenium coverages (Fig. 1 B) indicates that metal islands of an appropriate size are required.

The high hydrogen production rate on the illuminated 0.76 wt% Ru/TiO<sub>2</sub> was stable during the 48 h experiment.

In comparing the above results to those published earlier for platinumized TiO<sub>2</sub> [10], different optimum metal coverages (0.76 and 0.22 wt%, respectively) were

found in both cases for the highest active materials ( $\text{TiO}_2$  was prepared the same way). Hence the optimum coverage depends on the quantity of the photodeposited precious metal. Therefore, the optimization of metal content needs to be done for every particular metal when supported on  $\text{TiO}_2$ .

The influence of the solution  $pH$  on hydrogen evolution rates is shown in Fig. 3. It is seen that at higher  $pH$  (11.3 and 14.0) the hydrogen production is slightly higher, but is not stable with time. The best stability is obtained without any NaOH added to the slurry ( $pH$  3.9). The effect of  $pH$  on hydrogen photoproduction from Ru/ $\text{TiO}_2$  in water-methanol is complex and no conclusion can be drawn on the basis of the above results. It is possible that the addition of NaOH results both in a change of the ruthenium state in the solution as well as a change of the mechanism of water splitting and methanol oxidation.

Ruthenium distribution on the surface of  $\text{TiO}_2$  particles was observed with SEM; the images are shown in Figs. 4 and 5. The micrographs were performed for samples covered with 0.08 and 0.76 wt% Ru prepared under the usual reaction conditions, i.e. during the process of hydrogen photogeneration. Figs. 4 A and 5 A consist of two different micrographs: the usual SEI (secondary electron image) and electron probe microanalysis along the axis depicted on the figures. The microprobe analysis was performed using an electron beam of energy sufficient for electron excitation of ruthenium ( $L_\alpha$  ruthenium radiation was analysed). It is seen that the base lines of the Ru-distribution are raised on the catalyst particles showing the metal deposition on the whole surface. However, the peaks indicate the nonhomogeneity of the ruthenium deposits, i.e. the existence of smaller and bigger metal islets. Moreover, the metal islets are bigger for higher metal coverages (compare Figs. 4 A and 5 A). The nonhomogeneity of Ru-distribution is clearly shown on the images of line-by-line electron microprobe analysis (see Figs. 4 B and 5 B; a small white dot indicates the existence of agglomerates of at least 500 Ru atoms).

Fig. 5 C represents an AEI (adsorbed electron image) of the particle shown in Figs. 5 A and 5 B. Here the ruthenium islets are represented by black spots. It is evident that the black spots in Fig. 5 C correspond to the white ones in Fig. 5 A. Therefore, the distribution of ruthenium islets on the  $\text{TiO}_2$  surface can be roughly determined from SEI. Figs. 6 A and 6 B show SEI's for other particles of 0.76 wt% Ru/ $\text{TiO}_2$  and 0.08 wt% Ru/ $\text{TiO}_2$ . The graphs are sharper than those shown in Figs. 4 A and 5 A because of a magnification 4 times lower ( $1\ 000\times$ ). Small, white, round Ru islets are easy to observe.

## Acknowledgments

The authors thank Mr. Karol Jozwiak from The Technical University in Poznan, Poland, for performing SEM and electron microprobe analysis.

## References

- [1] See e.g. Sato S., White J. M. (1981) *J. Catal.* **69**: 128; Oosawa J. (1984) *J. Chem. Soc. Faraday Trans. 1* **80**: 1507
- [2] Zielinski S., Sobczynski A. (1986) *Acta Chim. Hung.* **21**: 305
- [3] Kiwi J., Graetzel M. (1984) *J. Phys. Chem.* **88**: 1302
- [4] Koudelka M., Sanchez J., Augustynski J. (1982) *J. Phys. Chem.* **86**: 4277
- [5] Kraeutler B., Bard A. J. (1978) *J. Am. Chem. Soc.* **100**: 1694



- [6] Sakata T., Kawai T. (1981) *Nouv. J. Chim.* **5**: 279
- [7] Borgarello E., Kiwi J., Pelizzetti E., Vicsa M., Graetzel M. (1981) *J. Am. Chem. Soc.* **103**: 6324
- [8] Yamaguti K., Sato S. (1985) *J. Chem. Soc. Faraday Trans. 1* **81**: 1237
- [9] Cameron R. E., Bocarsly A. B. (1986) *Inorg. Chem.* **25**: 2910
- [10] Sobczynski A. (1987) *J. Molec. Catal.* **39**: 43
- [11] Sobczynski A., Bard A. J., Campion A., Fox M. A., Mallouk T. E., Webber S. E., White J. M. (1987) *J. Phys. Chem.* **91**: 3319
- [12] Borgarello E., Harris R., Serpone N. (1985) *Nouv. J. Chim.* **9**: 743
- [13] Borgarello E., Serpone N., Emo G., Harris R., Pelizzetti E., Minero C. (1986) *Inorg. Chem.* **25**: 4499
- [14] Sakata T., Kawai T. (1980) *Nature (London)* **289**: 158
- [15] Miller D. S., Bard A. J., McLendon G., Ferguson J. (1981) *J. Am. Chem. Soc.* **103**: 5336
- [16] John M. R. S., Furgala A. J., Sammels A. F. (1983) *J. Phys. Chem.* **87**: 801
- [17] Yesodharan E., Graetzel M. (1983) *Helv. Chim. Acta* **66**: 2145
- [18] Yesodharan E., Yesodharan S., Graetzel M. (1984) *Solar Energy Mater.* **10**: 287
- [19] Chen B. H., White J. M. (1982) *J. Phys. Chem.* **86**: 3534
- [20] Fang S. M., Chen B. H., White J. M. (1982) *J. Phys. Chem.* **86**: 3126
- [21] Cranston R. W., Inkley F. A. (1957) *Adv. Catal.* **9**: 143
- [22] Sobczynski A., Zielinski S. (in preparation)
- [23] See e.g. Bard A. J. (1979) *J. Photochem.* **10**: 50
- [24] Kawai M., Kawai T., Naito S., Tamaru K. (1984) *Phys. Chem. Lett.* **110**: 58
- [25] Pichat P., Herrmann J. M., Disdier J., Courbon M., Mozzanega M. N. (1981) *Nouv. J. Chim.* **5**: 627
- [26] Pichat P. (1987) *Nouv. J. Chim.* **11**: 135
- [27] Pichat P., Mozzanega M. N., Disdier J., Herrmann J. M. (1982) *Nouv. J. Chim.* **6**: 559
- [28] Ko E. J., Wagner J. (1984) *J. Chem. Soc. Chem. Comm.*: 1274
- [29] Matsumura M., Harimoto M., Ichara T., Tsubomura H. (1984) *J. Phys. Chem.* **88**: 1984

*Received September 7, 1987. Accepted November 23, 1987*